CHAOS
Theory and Applications
in Applied Sciences and Engineering

e-ISSN: 2687-4539
RESEARCH ARTICLE
Vol.5 / No.2 / 2023 / pp.90-104
https://doi.org/10.51537/chaos.1214284

Bifurcation Analysis and 0-1 Chaos Test of a Discrete T System

Sarker Md. Sohel Rana *,[1]
*Department of Mathematics, University of Dhaka, Dhaka, 1000, Bangladesh.

ABSTRACT This study examines discrete-time T system. We begin by listing the topological divisions of the system's fixed points. Then, we analytically demonstrate that a discrete T system sits at the foundation of a Neimark Sacker(NS) bifurcation under specific parametric circumstances. With the use of the explicit Flip-NS bifurcation criterion, we establish the flip-NS bifurcation's reality. Center manifold theory is then used to establish the direction of both bifurcations. We do numerical simulations to validate our theoretical findings. Additionally, we employ the 0-1 test for chaos to demonstrate whether or not chaos exists in the system. In order to stop the system's chaotic trajectory, we ultimately employ a hybrid control method.

KEYWORDS
T system
Stability
Bifurcations
Chaos Control

INTRODUCTION

The nonlinear differential systems, including those in engineering, economy, physics, biology, chemistry, and other domains, have been explored from both theoretical and potential practical perspective. The feature of sensitivity to the beginning circumstances is frequently seen in nonlinear systems (some authors consider this property sufficient for a system to be chaotic). One of the first examples of a 3-D continuous dynamical system using numerical simulations that illustrate the property of sensitivity to initial conditions is the Lorenz system (Lorenz 1963).

The Rayleigh-Benard experiment is the Lorenz system's physical implementation. A dynamical model for meteorology was developed using the system, which was derived from the hydrodynamical Navier-Stokes equations. Scientists have looked into numerous 3-D chaotic systems as a result of his classically innovative work. After a decade, Rössler (1976) made the discovery of a 3-D chaotic system that had been built up while studying a chemical reaction. The discovery of numerous 3-D chaotic systems was made possible by these classical pioneering works on chaotic systems. Attempting to convert the Lorenz system from a stable to a chaotic condition (concept known as anticontrol of chaos), Lü *et al.* (2002) and Ueta and Chen (2000) constructed new critical chaotic systems by anti-control technique in Lorenz system (Lorenz 1963) which were known as Lü system and Chen's system respectively.

Manuscript received: 4 December 2022,
Revised: 20 April 2023,
Accepted: 22 May 2023.

[1] srana.mthdu@gmail.com (**Corresponding Author**)

Qualitative analyses of these empirical works found many dynamical properties including local bifurcations, chaotic, periodic, quasi-periodic orbits and route to chaos. They also obtained supercritical and sub-critical bifurcations conditions around positive equilibrium. In Sachdev and Sarathy (1994), a nonlinear system resulting from a nuclear spin generator is explored and contrasted with the Lorenz system. The T system, which Tigan (Tigan 2005) explored, is a novel chaotic system deriving from the Lorenz system. The system T exhibits a more complicated dynamics than the Lü system because it offers greater flexibility in selecting the system's parameters. To improve the chaotic system's complexity and the accuracy of the weak signal detection, a novel 3-D chaotic system studied (Luo *et al.* 2020). A 3-D jerk system dynamics examined in (Kengne *et al.* 2016), which can be utilized as an analog simulator for experiments made in a lab. This work investigated several dramatic and uncommon bifurcation situations, such as those with multiple attractors, symmetry-recovering crises, and basins of attraction for a variety of coexisting attractors. These applications provide justification for the creation of new chaotic systems. Numerous fields, ranging from ecology (Tang and Chen 2003) and physics (El Naschie 2003), encounter nonlinear dynamics.

We recall some applications of such systems in biological systems, secure communication, information processing (see, for example, (Babloyantz *et al.* 1985; Chen and Dong 1998; Chen 1999; Pecora and Carroll 1991; Rabinovich and Abarbanel 1998; Yang and Chua 1997)). A numerous number of scholars have been given attention and investigated extensively system's bifurcation in continuous dynamical system, but a little works have been studied in system's bifurcations in discrete dynamical system. However, a lot of exploratory works have been suggested that discrete-time

models are more suitable compared to differential equation model as discrete-time model reveal rich chaotic dynamics and give effective computational models for numerical simulations (Chakraborty *et al.* 2020; Li and He 2019; Liu and Li 2021; Rana 2019b,a; Zhao 2021; Liu and Li 2021; Zhang *et al.* 2022; Fei *et al.* 2021; Singh and Deolia 2021). These studies investigated unexpected characteristics, such as the occurrence of (flip-NS) bifurcations and chaotic events, using either numerical methods or center manifold theory applications. In fact, these studies solely focused on 2-D discrete systems.

A limited number of contributions have recently been made to the study of the dynamics of 3-D discrete systems (Khan and Javaid 2021; Abdelaziz *et al.* 2020; Din and Ishaque 2019; Feng *et al.* 2021; Hu *et al.* 2014; Ishaque *et al.* 2019; Qin *et al.* 2016; Khan *et al.* 2021; Xin *et al.* 2010). For example, a discrete-time SIR epidemic models discussed in (Abdelaziz *et al.* 2020; Khan *et al.* 2021; Hu *et al.* 2014), in (Xin *et al.* 2010) the authors investigated discrete financial system and in (Qin *et al.* 2016), the authors studied discrete chaotic system.

The explicit Flip-NS bifurcation criterion, center manifold theory, and bifurcation theory were all used by the researchers in these works to focus their efforts on figuring out the direction and stability of Flip and NS bifurcation. The studies in (Khan and Javaid 2021; Din and Ishaque 2019; Ishaque *et al.* 2019) investigated discrete population models. In (Feng *et al.* 2021), the authors explored NS bifurcation for discrete food chain model. For the existence of flip and NS bifurcations, these research solely employed the explicit (Flip-NS bifurcaton) criteria and numerical simulations. In nonlinear field research, the chaos theory has recently attracted a lot of attention.

In light of the aforementioned research projects, we express our interest in studying at 3-D T system (Tigan 2005):

$$\begin{aligned} \dot{x} &= a(y-x) \\ \dot{y} &= (c-a)x - axz \\ \dot{z} &= xy - bz \end{aligned} \tag{1}$$

In system (1), $x, y, z \in \mathbb{R}$ are the state variables with parameters $a, b, c \in \mathbb{R}$ and $a \neq 0$. The parameters $a, b, c \in \mathbb{R}^+$ in the system represent the Prandal number, the Rayleigh number, and some physical proportions of the region under study and for more description of these parameters we refer (Sparrow 2012). Diverse perspectives were used to study the T system: dynamics (Jiang *et al.* 2010), chaos control (Yong and Zhen-Ya 2008), anti-synchronization (Vaidyanathan and Rajagopal 2011). Secure communications might benefit from the system (1) (Li *et al.* 2009; Sundarapandian 2011). The T system undergoes a Hopf bifurcation and possesses a strange chaotic attractor (Jiang *et al.* 2010).

A continuous-time differential equation can be discretized in a variety of ways, but the fourth-order Runge-Kutta approach and the forward Euler scheme are the most straightforward. The discrete systems' features can change significantly from those of the original continuous ones since the forward Euler technique uses first-order precision to solve approximation differential equation solutions. However, a big step size ensures low stability of the selected Euler integrator, which means all of the impacts we see may have nothing to do with the characteristics of the original continuous system. This intentionally induced instability of the finite-difference system is where the chaotic regimes mostly develop. How the forward Euler scheme affects the capabilities of continuous systems is something we are interested in. Our present work is looking at a discrete-time system that is built on the continuous-time 3D T system. Applying forward Euler scheme, the discrete form of (1) is given by

$$\begin{pmatrix} x \\ y \\ z \end{pmatrix} \longrightarrow \begin{pmatrix} x + \delta(a(y-x)) \\ y + \delta((c-a)x - axz) \\ z + \delta(xy - bz) \end{pmatrix} \tag{2}$$

We are motivated to investigate the T system in discrete form because of the interest in studying it. The discrete T system differs from the continuous one in both characteristics and structure, according to analysis. The Flip and NS bifurcations play an significant role for generation of critical chaotic dynamics in discrete system and trigger a route to chaos. The objective of this work is to analyze systematically the conditions for occurence of flip and NS bifurcations by using an explicit Flip-NS bifurcation criterion and to determine the stability and direction of both bifurcations by the applications of bifurcation theory.

The structure of this study is as follows. The local stability requirements of possible fixed points are examined in Section 2. In Section 3, we theoretically examine whether the system (2) experiences a Flip or NS bifurcation under a certain parametric condition. To support the conclusions of our analytical work, we numerically show system dynamics in Section 4 together with bifurcation diagrams, phase portraits, and MLEs. There is also a $0-1$ chaotic test method offered. In Section 5, we put a hybrid control technique into practice to stabilize the uncontrolled system's chaos. We provide a brief summary in Section 6.

LOCAL DYNAMICS

The fixed points of the system (2) are the solutions of the following system of non-linear equations:

$$\begin{aligned} x &= x + \delta(a(y-x)) \\ y &= y + \delta((c-a)x - axz) \\ z &= z + \delta(xy - bz) \end{aligned} \tag{3}$$

By some algebraic computation, we obtain the following lemma.

Lemma 1 *(i) For any parameter values, the system (2) has only one fixed point* $E_0 = (0,0,0)$*, (ii) if* $c > a$*, the system (2) has three fixed points* $E_0 = (0,0,0)$*, and* $E_\pm = (x^\pm, y^\pm, z^\pm) = \left(\pm\sqrt{\frac{b}{a}(c-a)}, \pm\sqrt{\frac{b}{a}(c-a)}, \frac{c-a}{a}\right)$.

Given at fixed point $E(x,y,z)$, the Jacobian matrix of the system (2) and its characteristic equation are as follows

$$J(E) = \begin{pmatrix} 1-a\delta & a\delta & 0 \\ -(a-c+az)\delta & 1 & -ax\delta \\ y\delta & x\delta & 1-b\delta \end{pmatrix} = (j_{kl}), \quad k,l = 1,2,3 \tag{4}$$

and

$$P(\mu) := \mu^3 + \vartheta_2\mu^2 + \vartheta_1\mu + \vartheta_0 = 0 \tag{5}$$

where,

$$\vartheta_2 = -tr(J),$$
$$\vartheta_1 = \begin{vmatrix} j_{11} & j_{12} \\ j_{21} & j_{22} \end{vmatrix} + \begin{vmatrix} j_{22} & j_{23} \\ j_{32} & j_{33} \end{vmatrix} + \begin{vmatrix} j_{11} & j_{13} \\ j_{31} & j_{33} \end{vmatrix},$$
$$\vartheta_0 = -|J|.$$

We first provide the following lemma regarding the necessary and sufficient criteria for stability around fixed point of system (2) in order to study the nature of the system around fixed point $E(x, y, z)$.

Lemma 2 *(Camouzis and Ladas 2007) Suppose that $\vartheta_2, \vartheta_1, \vartheta_0 \in \mathbb{R}$.Then, the necessary and sufficient conditions for all roots μ of the equation*

$$\mu^3 + \vartheta_2\mu^2 + \vartheta_1\mu + \vartheta_0 = 0$$

to satisfy $|\mu| < 1$ are
$|\vartheta_2 + \vartheta_0| < 1 + \vartheta_1, |\vartheta_2 - 3\vartheta_0| < 3 - \vartheta_1$, *and* ${\vartheta_0}^2 + \vartheta_1 - \vartheta_0\vartheta_2 < 1$.

Now, the local dynamics of system (2) around fixed points E_0 and E_+ are as follows.

At E_0, the Jacobian matrix $J(E_0)$ have eigenvalues $\mu_1 = 1 - b\delta, \mu_{2,3} = \frac{1}{2}\left(2 - a\delta \pm \sqrt{\delta^2(-3a^2 + 4ac)}\right)$, where $\mu_{2,3}$ satisfy the equation

$$\mu^2 - (2 - a\delta)\mu + (1 - a\delta + (a^2 - ac)\delta^2) = 0.$$

We obtain the topological classification of E_0 presented in the following Lemma.

Lemma 3 *If $c < a$, the fixed point E_0 is a*
– sink if $(i) - 3a^2 + 4ac \geq 0, \delta < \min\left\{\frac{2}{b}, \frac{a-\sqrt{-3a^2+4ac}}{a^2-ac}\right\}$,
$(ii) - 3a^2 + 4ac < 0, \delta < \min\left\{\frac{2}{b}, \frac{1}{a-c}\right\}$,
– source if $(iii) - 3a^2 + 4ac \geq 0, \delta > \max\left\{\frac{2}{b}, \frac{a-\sqrt{-3a^2+4ac}}{a^2-ac}\right\}$,
$(iv) - 3a^2 + 4ac < 0, \delta > \max\left\{\frac{2}{b}, \frac{1}{a-c}\right\}$,
– non-hyperbolic if $(v) - 3a^2 + 4ac \geq 0, \delta = \frac{2}{b}$, *or* $\delta = \frac{a\pm\sqrt{-3a^2+4ac}}{a^2-ac}$,
$(vi) - 3a^2 + 4ac < 0, \delta = \frac{1}{a-c}$.

Let,

$$FB_{E_0} = \left\{(a, b, c, \delta) : \delta = \frac{a \pm \sqrt{-3a^2 + 4ac}}{a^2 - ac}, \quad \delta \neq \frac{2}{b}, \quad -3a^2 + 4ac \geq 0\right\}$$

and

$$NSB_{E_0} = \left\{(a, b, c, \delta) : \delta = \frac{1}{a - c}, -3a^2 + 4ac < 0\right\},$$

then system (2) encounters a flip (NS) bifurcation at E_0 if parameters change in small vicinity of FB_{E_0} (NSB_{E_0}).

At E_+, we rewrite the equation (5) as

$$P(\mu) := \mu^3 + \kappa_2\mu^2 + \kappa_1\mu + \kappa_0 = 0. \tag{6}$$

where,

$$\begin{aligned} \kappa_2 &= -3 + \delta(a + b), \\ \kappa_1 &= 3 - 2a\delta + b\delta(-2 + c\delta), \\ \kappa_0 &= -1 - 2a^2b\delta^3 + b(\delta - c\delta^2) + a(\delta + 2bc\delta^3) \end{aligned} \tag{7}$$

Following is the Lemma for stability requirement of E_+.

Lemma 4 *The fixed point E_+ of system (2) is locally asymptotically stable if and only if the coefficients $\kappa_2, \kappa_1, \kappa_0$ of (6) satisfy*
$|\kappa_2 + \kappa_0| < 1 + \kappa_1, \quad |\kappa_2 - 3\kappa_0| < 3 - \kappa_1$, *and* ${\kappa_0}^2 + \kappa_1 - \kappa_0\kappa_2 < 1$.

ANALYSIS OF BIFURCATIONS

This part will focus to recapitulate the conditions for stability and direction of flip and NS bifurcations of system (2) around fixed points E_0 and E_+ by using an explicit Flip-NS bifurcation criterion without computing the eigenvalues of the respective system and bifurcation theory (Kuznetsov 2013; Wen 2005; Yao 2012). We take δ as bifurcation parameter, otherwise stated.

NS bifurcation around E_0

Suppose that parameters $(a, b, c, \delta) \in NSB_{E_0}$, then the eigenvalues of system (2) are

$$\mu_1 = 1 - b\delta, \quad \mu_{2,3} = \alpha \pm i\beta \tag{8}$$

where $\alpha = 1 - \frac{a\delta}{2}$ and $\beta = \delta\sqrt{3a^2 - 4ac}$.

Let, $\delta = \delta_{NS} = \frac{1}{a-c}$, then we have

$$|\mu_{2,3}(\delta_{NS})| = \sqrt{(1 - a\delta_{NS} + (a^2 - ac)\delta_{NS}^2)} = 1, \quad \mu_1(\delta_{NS}) = 1 - \frac{b}{a - c} \tag{9}$$

and

$$\frac{d\,|\mu_i(\delta)|}{d\delta}|_{\delta=\delta_{NS}} = \frac{a}{2} \neq 0, i = 2, 3 \tag{10}$$

Moreover,

$$\frac{a}{a - c} \neq 2, 3 \tag{11}$$

implies that $\mu_{2,3}^k \neq 1, \quad k = 1, 2, 3, 4$. We write the system (2) as

$$X = A(\delta)X + F \tag{12}$$

where $A(\delta) = J(E_0)$ and $F = (0, -axz\delta, xy\delta)^T$ with $\delta = \delta_{NS}$. It is possible to express the system (12) as

$$X_{n+1} = AX_n + \frac{1}{2}B(X_n, X_n) + \frac{1}{6}C(X_n, X_n, X_n) + O\left(X_n^4\right)$$

where,

$$B(x, y) = \begin{pmatrix} B_1(x, y) \\ B_2(x, y) \\ B_3(x, y) \end{pmatrix} \quad \text{and} \quad C(x, y, u) = \begin{pmatrix} C_1(x, y, u) \\ C_2(x, y, u) \\ C_3(x, y, u) \end{pmatrix} \tag{13}$$

are the symmetric multi-linear functions of $x, y, z, u \in \mathbb{R}^3$ and defined by

$$B_i(x, y) = \sum_{j,k=1}^{3} \frac{\partial^2 F_i(v, \delta)}{\partial v_j \partial v_k}\Big|_{v=0} x_j y_k,$$

$C_i(x,y,u) = \sum_{j,k,l=1}^{3} \frac{\partial^3 F_i(v,\delta)}{\partial v_j \partial v_k \partial v_l}\Big|_{v=0} x_j y_k u_l.$

In particular,

$$B(x,y) = \begin{pmatrix} 0 \\ -ax_3y_1\delta - ax_1y_3\delta \\ x_2y_1\delta + x_1y_2\delta \end{pmatrix} \quad \text{and} \quad C(x,y,u) = \begin{pmatrix} 0 \\ 0 \\ 0 \end{pmatrix} \tag{14}$$

Let $\zeta_1, \zeta_2 \in \mathbb{C}^3$ be two eigenvectors of $A(\delta_{NS})$ and $A^T(\delta_{NS})$ respectively such that

$$A(\delta_{\mathrm{NS}})\zeta_1 = \mu_2(\delta_{\mathrm{NS}})\zeta_1, \quad A^T(\delta_{\mathrm{NS}})\zeta_2 = \mu_3(\delta_{\mathrm{NS}})\zeta_2 \tag{15}$$

then after some algebraic calculation, we obtain

$$\zeta_1 = (\phi_1 + i\psi_1, 1, 0)^T \quad \text{and} \quad \zeta_2 = (\phi_2 + i\psi_2, 1, 0)^T$$

with $\phi_1 = \frac{a\delta}{2(a-c)\delta}, \psi_1 = \frac{-\beta}{2(a-c)\delta}$ and $\phi_2 = \frac{-a\delta}{2a\delta}, \psi_2 = \frac{-\beta}{2a\delta}$.

The standard inner product property $\langle \zeta_1, \zeta_2 \rangle = \sum_{i=1}^{3} \zeta_{1i}\overline{\zeta_{2i}}$ is applied to set the normalized vector $\zeta_2 = \xi\zeta_2$ so that $\langle \zeta_1, \zeta_2 \rangle = 1$ is obtained where $\xi = \xi_1 + i\xi_2$ with

$$\xi_1 = \frac{\phi_1\phi_2 + \psi_1\psi_2 + 1}{(\phi_1\phi_2 + \psi_1\psi_2 + 1)^2 + (\phi_2\psi_1 - \phi_1\psi_2)^2},$$
$$\xi_2 = \frac{\phi_2\psi_1 - \phi_1\psi_2}{(\phi_1\phi_2 + \psi_1\psi_2 + 1)^2 + (\phi_2\psi_1 - \phi_1\psi_2)^2}.$$

Now, decomposing the vector $X \in \mathbb{R}^3$ as $X = z\zeta_1 + \bar{z}\bar{\zeta_1}$ by considering δ vary near to δ_{NS} and for $z \in \mathbb{C}$. Obviously, $z = \langle \zeta_2, X \rangle$. So, we derive the transformed form of system (12) for $|\delta|$ close to δ_{NS} as follows:

$$z \longmapsto \mu(\delta)z + \widehat{g}(z, \bar{z}, \delta) \tag{16}$$

where $\mu(\delta) = (1 + \widehat{\varphi}(\delta))e^{i\theta(\delta)}$ with $\widehat{\varphi}(\delta_{\mathrm{NS}}) = 0$ and $\widehat{g}(z, \bar{z}, \delta)$ is a smooth complex-valued function. Then we obtain $\widehat{g}(z, \bar{z}, \delta) = \sum_{k+l\geq 2} \frac{1}{k!l!}\widehat{g}_{kl}(\delta) z^{k-l}$ with $\widehat{g}_{kl} \in \mathbb{C}, k, l = 0, 1, \ldots$.

The coefficients $\widehat{g}_{kl}$ are determined via multilinear symmetric vector functions:

$$\begin{aligned}
&\widehat{g}_{20}(\delta) = \langle \zeta_2, B(\zeta_1, \zeta_1) \rangle, \widehat{g}_{11}(\delta) = \langle \zeta_2, B(\zeta_1, \bar{\zeta_1}) \rangle, \\
&\widehat{g}_{02}(\delta) = \langle \zeta_2, B(\bar{\zeta_1}, \bar{\zeta_1}) \rangle, \\
&\widehat{g}_{21}(\delta) = \langle \zeta_2, C(\zeta_1, \zeta_1, \bar{\zeta_1}) \rangle + 2\left\langle \zeta_2, B\left(\zeta_1, (I_n - A)^{-1} B(\zeta_1, \bar{\zeta_1})\right)\right\rangle \\
&\qquad + \left\langle \zeta_2, B\left(\bar{\zeta_1}, \left(\mu_2^2 I_n - A\right)^{-1} B(\zeta_1, \zeta_1)\right)\right\rangle + \frac{(1-2\mu_2)\mu_3}{1-\mu_2}\widehat{g}_{20}\widehat{g}_{11} \\
&\qquad + \frac{2}{1-\mu_2}|\widehat{g}_{11}|^2 + \frac{\mu_2}{\mu_2^3 - 1}|\widehat{g}_{02}|^2.
\end{aligned} \tag{17}$$

with $\delta = \delta_{\mathrm{NS}}$.

After some tedious calculation, we get

$$\begin{aligned}
&\widehat{g}_{20}(\delta_{\mathrm{NS}}) = 0, \widehat{g}_{11}(\delta_{\mathrm{NS}}) = 0, \widehat{g}_{02}(\delta_{\mathrm{NS}}) = 0, \\
&\widehat{g}_{21}(\delta_{\mathrm{NS}}) = \frac{-2a\delta_{\mathrm{NS}}}{b\left(\Phi_4^2 + \Psi_4^2\right)}\left[(\Phi_3\Phi_4 + \Psi_3\Psi_4) + i(\Phi_4\Psi_3 - \Phi_3\Psi_4)\right]
\end{aligned} \tag{18}$$

where

$$\begin{aligned}
\Phi_4 &= -1 + \alpha^2 - \beta^2 + b\delta, \\
\Psi_4 &= 2\alpha\beta, \\
\Phi_3 &= \Phi_1\Phi_2 - \Psi_1\Psi_2, \\
\Psi_3 &= \Phi_2\Psi_1 + \Phi_1\Psi_2, \\
\Phi_2 &= \phi_1(-2 + 2\alpha^2 - 2\beta^2 + 3b\delta), \\
\Psi_2 &= 4\phi_1\alpha\beta - b\psi_1\delta, \\
\Phi_1 &= \phi_1\xi_1 + \psi_1\xi_2, \\
\Psi_1 &= \psi_1\xi_1 - \phi_1\xi_2.
\end{aligned}$$

Then using coefficient of the critical normal form

$$l_1(\delta_{\mathrm{NS}}) = \mathrm{Re}\left(\frac{\mu_3\widehat{g}_{21}}{2}\right) - \mathrm{Re}\left(\frac{(1-2\mu_2)\mu_3^2}{2(1-\mu_2)}\widehat{g}_{20}\widehat{g}_{11}\right) - \frac{1}{2}|\widehat{g}_{11}|^2 - \frac{1}{4}|\widehat{g}_{02}|^2 \tag{19}$$

we obtain $l_1(\delta_{\mathrm{NS}}) = \frac{-a\delta_{\mathrm{NS}}}{b\left(\Phi_4^2 + \Psi_4^2\right)}(\Phi_6\Phi_4 + \Psi_6\Psi_4)$ where

$$\begin{aligned}
\Phi_5 &= \alpha\Phi_1 + \beta\Psi_1, \\
\Psi_5 &= \alpha\Psi_1 - \beta\Phi_1, \\
\Phi_6 &= \Phi_2\Phi_5 - \Psi_2\Psi_5, \\
\Psi_6 &= \Phi_2\Psi_5 + \Phi_5\Psi_2.
\end{aligned}$$

The following theorem can be used in conjunction with the preceding description to demonstrate the direction and stability of the NS bifurcation.

Theorem 1 *Suppose (11) holds and $l_1(\delta_{NS}) \neq 0$, then NS bifurcation emerges at fixed point $E_0(0,0,0)$ for system (2) if the δ changes its value in small neighbourhood of NSB_{E_0}. Additionally, there exists an attractive (resp. repelling) smooth closed invariant curve bifurcate from E_+ if $l_1(\delta_{NS}) < 0$ (resp. $l_1(\delta_{NS}) > 0$) and the bifurcation is sub-critical (resp. super-critical).*

Bifurcation Analysis around E_+

Flip Bifurcation: Existence condition To investigate the existence of flip bifurcation, we will use Lemma in (Yao 2012).

Lemma 5 *The flip bifurcation of system (2) takes place around fixed point $E_+ = \left(\sqrt{\frac{b}{a}(c-a)}, \sqrt{\frac{b}{a}(c-a)}, \frac{c-a}{a}\right)$ at $\delta = \delta_F$ if and only if*

$1 - \kappa_1 + \kappa_0(\kappa_2 - \kappa_0) > 0,$
$1 + \kappa_1 - \kappa_0(\kappa_2 + \kappa_0) > 0,$
$1 + \kappa_2 + \kappa_1 + \kappa_0 > 0,$
$1 - \kappa_2 + \kappa_1 - \kappa_0 = 0,$
$1 + \kappa_0 > 0,$
$1 - \kappa_0 > 0,$

and $\frac{\sum_{i=1}^{n}(-1)^{n-i}\iota_i'}{\sum_{i=1}^{n}(-1)^{n-i}(n-i+1)\iota_{i-1}} = \frac{\kappa_2' - \kappa_1' + \kappa_0'}{3 - 2\kappa_2 + \kappa_1} \neq 0,$

where $\kappa_2, \kappa_1, \kappa_0$ are given as in (7) and $\kappa_i' = \frac{d\kappa_i}{d\delta}|_{\delta=\delta_F}$ with

$\delta_F = \frac{-c}{3a^2-3ac} + \frac{6a^3+6a^2(b-c)-6abc+bc^2}{3a(a-c)\Gamma_1} + \frac{\Gamma_1}{3ab(a-c)}$,
$\Gamma_1 = \sqrt[3]{-54a^4b^2 + 99a^3b^2c + 9ab^3c^2 - b^3c^3 - 9a^2b^2c(b+5c) + 3\sqrt{3}\sqrt{\Gamma_2}}$,
$\Gamma_2 = -a^2b^3(a-c)^2(8a^5 + b^2(b-4c)c^2 - 4a^4(21b+2c) + 12a^3b(2b+13c) + \Gamma_3)$,
$\Gamma_3 = 2ab^2c(-4b+19c) + a^2b(8b^2 - 60bc - 71c^2)$.

Define the set

$$FB_{E_+} = \{(a,b,c,\delta) : \delta = \delta_F, a, b, c > 0\}.$$

If system parameters value vary in a small vicinity of FB_{E_+}, one of the eigenvalue of (6) is $\mu_3(\delta_F) = -1$ and other two are $|\mu_{1,2}(\delta_F)| \neq \pm 1$, and then system (2) underlies a flip bifurcation around E_+.

Flip Bifurcation: Direction and Stability We choose parameter $(a,b,c,\delta) \in FB_{E_+}$ and let $\delta = \delta_F$, then the eigenvalues of $J(E_+)$ are:

$$\mu_1(\delta_F) = -1, \quad |\mu_i(\delta_F)| \neq \pm 1, i = 2,3 \tag{20}$$

Next, we set $\hat{x} = x - x^+, \hat{y} = y - y^+, \hat{z} = z - z^+$, $A(\delta_F) = J(E_+)$ and transfer the fixed point E_+ of system (2) to the origin. Since symmetric multi-linear functions are not associated with fixed point, the bi-linear and trilinear functions for flip bifurcation will remain unchanged as in (14).

Consider two eigenvectors $\eta_1, \eta_2 \in \mathbb{R}^3$ of A for eigenvalue $\mu_1(\delta_F) = -1$ such that

$$A(\delta_F)\eta_1 = -\eta_1, \quad A^T(\delta_F)\eta_2 = -\eta_2, \quad \langle \eta_2, \eta_1 \rangle = 1.$$

Then the coefficient of normal form is

$$l_2(\delta_F) = \frac{1}{6}\langle \eta_2, C(\eta_1,\eta_1,\eta_1)\rangle - \frac{1}{2}\left\langle \eta_2, B\left(\eta_1, (A-I)^{-1}B(\eta_1,\eta_1)\right)\right\rangle \tag{21}$$

In light of the aforementioned investigation, we provide the following conclusion with regard to the stability and direction of the flip bifurcation.

Theorem 2 *Suppose (20) holds well and $l_2(\delta_F) \neq 0$ for the fixed point $E_+(x^+, y^+, z^+)$. Then the system (2) encounters a flip bifurcation at E_+ if $l_2(\delta_F) \neq 0$ and δ fluctuates its value in a limited proximity of bifurcation point. Moreover, stable (resp., unstable) period-2 orbits split off from E_+ if $l_2(\delta_F)$ is positive (resp., negative).*

NS Bifurcation: Existence condition We will use the explicit Flip-NS bifurcation criterion (Wen 2005; Yao 2012) for the existence of NS bifurcation and the subsequent lemma will give the necessary and sufficient parametric conditions for which system (2) underlies NS bifurcation if bifurcation parameter δ passes its critical value.

Lemma 6 *The NS bifurcation of system (2) occurs around the fixed point E_+ at $\delta = \delta_{NS_+}$ if and only if*
$1 - \kappa_1 + \kappa_0(\kappa_2 - \kappa_0) = 0$,
$1 + \kappa_1 - \kappa_0(\kappa_2 + \kappa_0) > 0$,
$1 + \kappa_2 + \kappa_1 + \kappa_0 > 0$,
$1 - \kappa_2 + \kappa_1 - \kappa_0 > 0$,
$\frac{d}{d\delta}\left(1 - \kappa_1 + \kappa_0(\kappa_2 - \kappa_0)\right)_{\delta=\delta_{NS_+}} \neq 0$,
and $\cos\left(\frac{2\pi}{l}\right) \neq 1 - \frac{1+\kappa_2+\kappa_1+\kappa_0}{2(1+\kappa_0)}, l = 3,4,5,\ldots$

where $\kappa_2, \kappa_1, \kappa_0$ are given as in (7) with

$\delta_{NS_+} = \frac{1}{48a^2b(a-c)^2}\left(\frac{16abc(-a+c)-(8a^2b(a-c)^2(6a^3+6a^2(b-c)-6abc+bc^2))}{\Lambda_1} - 8\Lambda_1\right)$,
$\Lambda_1 = \sqrt[3]{\Lambda_2 + \Lambda_3 + 3\sqrt{3}\sqrt{\Lambda_4}}$,
$\Lambda_2 = -54a^10b^2 + 261a^9b^2c - 12a^4b^3c^5 + a^3b^3c^6 + 3a^5b^2c^4(13b + 15c)$,
$\Lambda_3 = 18a^7b^2c^2(2b+27c) - 9a^8b^2c(b+56c) - a^6b^2c^3(55b+234c)$,
$\Lambda_4 = -a^8b^3(a-c)^8(8a^5 + b^2(b-4c)c^2 - 4a^4(21b+2c) + 12a^3b(2b+13c) + \Lambda_5)$,
$\Lambda_5 = 2ab^2c(-4b+19c) + a^2b(8b^2 - 60bc - 71c^2)$.

Set

$$NSB_{E_+} = \{(a,b,c,\delta) : \delta = \delta_{NS_+}, a, b, c > 0\},$$

and for parameter perturbation in a small neighborhood of NSB_{E_+}, two roots (eigenvalues) of (6) are complex conjugate having modulus one and the magnitude of other root is not equal to one, then the system (2) experiences NS bifurcation around E_+.

NS Bifurcation: Direction and Stability This section will present the direction of NS bifurcation. We choose the fixed point E_+ of system (2) with arbitrary parameter $(a,b,c,\delta) \in NSB_{E_+}$. Let, $\delta = \delta_{NS_+}$, then the matrix $J(E_+)$ has the eigenvalues satisfying

$$|\mu_i(\delta_{NS_+})| = 1, i = 2,3 \tag{22}$$

and $\mu_1(\delta_{NS_+}) \neq 1$.

For eigenvalues $\mu_2(\delta_{NS_+})$ and $\mu_3(\delta_{NS_+})$, let $\tau_1, \tau_2 \in \mathbb{C}^3$ be two eigenvectors of $A(\delta_{NS_+})$ and $A^T(\delta_{NS_+})$ respectively such that

$$A\left(\delta_{\mathrm{NS}_+}\right)\tau_1 = \mu_2\left(\delta_{\mathrm{NS}_+}\right)\tau_1, A^T\left(\delta_{\mathrm{NS}_+}\right)\tau_2 = \mu_3\left(\delta_{\mathrm{NS}_+}\right)\tau_2, \quad \langle \tau_2, \tau_1\rangle = \textstyle\sum_{i=1}^3 \overline{\tau_{2i}}\tau_{1i} = 1 \tag{23}$$

The coefficient $l_3(\delta_{NS_+})$ calculated by (19) presents the direction and stability of NS bifurcation which has been stated in the following theorem.

Theorem 3 *Suppose (22) holds and $l_3(\delta_{NS_+}) \neq 0$ for the fixed point E_+. Then system (2) encounters NS bifurcation at E_+ if the δ fluctuates its value in a limited vicinity of NSB_{E_+}. Moreover, if $l_3(\delta_{NS_+}) < 0$ (resp. $l_3(\delta_{NS_+}) > 0$), a singular invariant closed curve bifurcates from E_+ that is attracting (resp., repelling) and the bifurcation is sub-critical (resp. super-critical).*

NUMERICAL SIMULATIONS

Using numerical simulations with the aid of bifurcation diagrams, phase portraits, and MLEs, we will confirm our theoretical conclusions for the system (2) in this section. The presence of chaos has been supported by the $0-1$ test algorithm. For the investigations of bifurcations, we will take different set of parameter values.

Example 1 *We take parameter values $a = 18, b = 12, c = 10$ and $0.1 \leq \delta \leq 0.1317$. By calculation, we find a fixed point $E_0 = (0,0,0)$ of system (2) and the bifurcation point is obtained as $\delta_{NS} = 0.125$. The Jacobian matrix J evaluated at E_0 have eigenvalues $\mu_1 = -0.5$ and $\mu_{2,3} = -0.125 \pm 0.9921575i$ with $|\mu_{2,3}| = 1$.*

Furthermore,

$$\frac{d\,|\mu_i(\delta)|}{d\delta}|_{\delta=\delta_{NS}} = \frac{a}{2} = 9 \neq 0, i = 2,3,$$

$$\frac{a}{a-c} = \frac{9}{4} \neq 2, 3.$$

So, the criterion for the existence of NS bifurcation are fulfilled with $(a, b, c, \delta) \in NSB_{E_0}$. *This confirms the correctness of Lemma 3. Therefore, a NS bifurcation occurs around fixed point* E_0 *if* δ *crosses its critical value* δ_{NS}.

Let $\zeta_1, \zeta_2 \in \mathbb{C}^3$ *be two complex eigenvectors of* $A(\delta_{NS})$ *and* $A^T(\delta_{NS})$ *corresponding to* $\mu_{2,3}$, *respectively. Therefore,*

$$\zeta_1 \sim (1.125 - 0.992157i, 1, 0)^T, \zeta_2 \sim (-0.5 - 0.440959i, 1, 0)^T.$$

For $\langle \zeta_1, \zeta_2 \rangle = 1$, *we can take normalized vector as* $\zeta_2 = \gamma\zeta_2$ *where,* $\gamma = 0.5 + 0.566947i$. *Then*

$$\zeta_1 \sim (1.125 - 0.992157i, 1, 0)^T, \zeta_2 \sim (-0.503953i, 0.5 + 0.566947i, 0)^T.$$

Also by (18) the Taylor coefficients are , $\widehat{g}_{20} = 0$, $\widehat{g}_{11} = 0$, $\widehat{g}_{02} = 0$, $\widehat{g}_{21} = 0.421875 - 0.797269i$.

From (19), we obtain the Lyapunov coefficient $l_2(\delta_{NS}) = -0.421875 < 0$. *As a result, the NS bifurcation is super-critical and the Theorem 1 conditions are satisfied.*

The NS bifurcation diagrams are displayed in Figure 1 (a) which reveal that the condition of stability for the positive fixed point E_0 *occurs when* $\delta < \delta_{NS}$, *loses its stability at* $\delta = \delta_{NS}$ *and there appears an attracting closed invariant curve when* $\delta > \delta_{NS}$. *The MLEs related to Figure 1 (a) are shown in Figure 1 (b). The non stability of system dynamics are justified with the sign of MLEs.*

The phase portraits of system (2) that correspond to the bifurcation diagram in Figure 1 (a) are plotted in Figure 2, explicitly illuminating the mechanism by which an invariant smooth closed curve splits from a stable fixed point E_0 *when* δ *varies close to its critical value. We noticed that NS bifurcations occurs at* $\delta = \delta_{NS}$ *(see in Figure 2(b)). When* $\delta > \delta_{NS}$, *there appears an invariant closed curve and further increasing of* δ, *NS bifurcation instigate a route to chaos.*

Example 2 *We take* $a = 5.2, b = 13.5, c = 6.5$, $0.14 \leq \delta \leq 0.1636$. *We obtain* $E_+ = (1.83712, 1.83712, 0.25)$ *and bifurcation point* $\delta_F = 0.1533$. *At* $\delta = \delta_F$, *the Jacobian matrix of system (2) takes the form*

$$A(\delta_F) = \begin{pmatrix} 0.202839 & 0.797161 & 0 \\ 0 & 1 & -1.46448 \\ 0.28163 & 0.28163 & -1.06955 \end{pmatrix}.$$

and the eigenvalues of $A(\delta_F)$ *are* $\mu_1 = -1$ *and* $\mu_{2,3} = 0.566644 \pm 0.375479i$ *with* $|\mu_{2,3}| = 0.679757$. *Moreover,*

$1 - \kappa_1 + \kappa_0 (\kappa_2 - \kappa_0) = 1.39612 > 0,$
$1 + \kappa_1 - \kappa_0 (\kappa_2 + \kappa_0) = 0.176862 > 0,$
$1 + \kappa_2 + \kappa_1 + \kappa_0 = 0.657564 > 0,$
$1 - \kappa_2 + \kappa_1 - \kappa_0 = 0,$
$1 + \kappa_0 = 1.46207 > 0,$
$1 - \kappa_0 = 0.53793 > 0,$
and
$\frac{\kappa_2' - \kappa_1' + \kappa_0'}{3 - 2\kappa_2 + \kappa_1} = 13.0463 \neq 0$

This shows that all requirements of Lemma 5 are validated with $(a, b, c, \delta) \in FB_{E_+}$. *Thus, the requirement for flip bifurcation's existence is confirmed and system (2) experience a flip bifurcation around* E_+ *at* $\delta = \delta_F$.

Next, let the two eigenvectors of $A(\delta_F)$ *corresponding to* $\mu_1(\delta_F) = -1$, *be* $\eta_1, \eta_2 \in \mathbb{R}^3$ *respectively. Then, we obtain*

$$\eta_1 \sim (-0.364586, 0.550125, 0.7512923)^T, \eta_2 \sim (-0.227729, -0.0461924, 0.972628)^T.$$

To set $\langle \eta_1, \eta_2 \rangle = 1$, *we can choose normalized vector as* $\eta_2 = \gamma\zeta_2$ *where,* $\gamma = 1.26848$. *Therefore,*

$$\eta_1 \sim (-0.364586, 0.550125, 0.751292)^T, \eta_2 \sim (-0.288871, -0.0585943, 1.23376)^T.$$

Then from (21), the Lyapunov coefficient $l_2(\delta_F) = 0.0397406 > 0$ *is obtained. This guarantees the appropriateness of Theorem 2.*

The diagrams of bifurcation shown in Figure 3 (a) express the stability of fixed point E_+ *when* δ *crosses bifurcation point. The MLEs and phase portraits of system (2) associated with Figure 3 (a) are shown in Figure 3 (b) and Figure 4 respectively which explicitly illustrate the mechanism of how period doublling phenomena leads to chaos.*

Example 3 *We choose* $0.06 \leq \delta \leq 0.11$, $a = 12, b = 12, c = 18$. *Then we find a fixed point* $E_+ = (2.44949, 2.44949, 0.5)$ *of system (2) and the bifurcation point is obtained as* $\delta_{NS_+} = 0.0671545$. *The Jacobian matrix is evaluated at* E_+ *is*

$$A(\delta_{NS}) = \begin{pmatrix} 0.194146 & 0.805854 & 0 \\ 0 & 1 & -1.97393 \\ 0.164494 & 0.164494 & 0.194146 \end{pmatrix},$$

and the eigenvalues of $A(\delta_{NS})$ *are* $\mu_1 = -0.16093$ *and* $\mu_{2,3} = 0.77461 \pm 0.632439i$ *with* $|\mu_{2,3}| = 1$.

Furthermore,
$1 - \kappa_1 + \kappa_0 (\kappa_2 - \kappa_0) = 0,$
$1 + \kappa_1 - \kappa_0 (\kappa_2 + \kappa_0) = 1.9482 > 0,$
$1 + \kappa_2 + \kappa_1 + \kappa_0 = 0.523323 > 0,$
$1 - \kappa_2 + \kappa_1 - \kappa_0 = 2.97805 > 0,$
$\frac{d}{d\delta}(1 - \kappa_1 + \kappa_0 (\kappa_2 - \kappa_0)) = -8.55995 \neq 0$
and
$1 - \frac{1 + \kappa_2 + \kappa_1 + \kappa_0}{2(1 + \kappa_0)} = 0.77461.$

From the resonance condition $\cos\left(\frac{2\pi}{l}\right) = 0.77461$, *we get* $l = \pm 9.17659$.

So, the criterion for the existence of NS bifurcation are fulfilled with $(a, b, c, \delta) \in NSB_{E_+}$. *This confirms the correctness of Lemma 6. Therefore, a NS bifurcation occurs around fixed point* E_+ *if* δ *crosses its critical value* δ_{NS_+}.

Let $\tau_1, \tau_2 \in \mathbb{C}^3$ *be two complex eigenvectors of* $A(\delta_{NS})$ *and* $A^T(\delta_{NS})$ *corresponding to* $\mu_{2,3}$, *respectively. Therefore,*

$$\tau_1 \sim (0.449192 - 0.489412i, 0.70765, 0.0808016 - 0.226728i)^T, \tau_2 \sim (0.117028 + 0.127506i, -0.265599 + 0.28938i, 0.903196)^T.$$

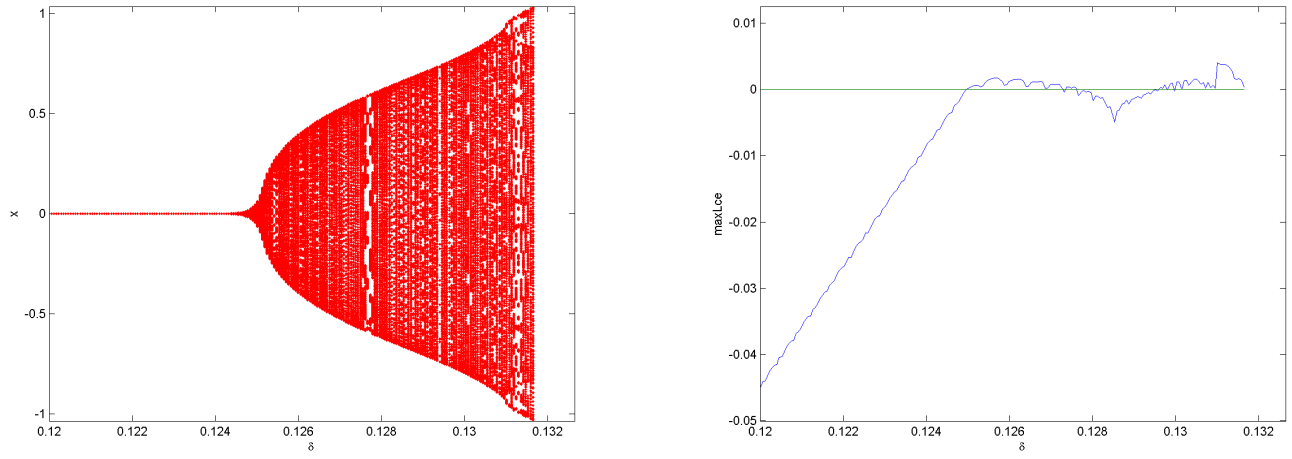

(a) (b)

Figure 1 NS Bifurcation Diagram: in (a) (δ, x) plane, (b) MLEs, $(x_0, y_0, z_0) = (0.93, 0.93, 0.33)$.

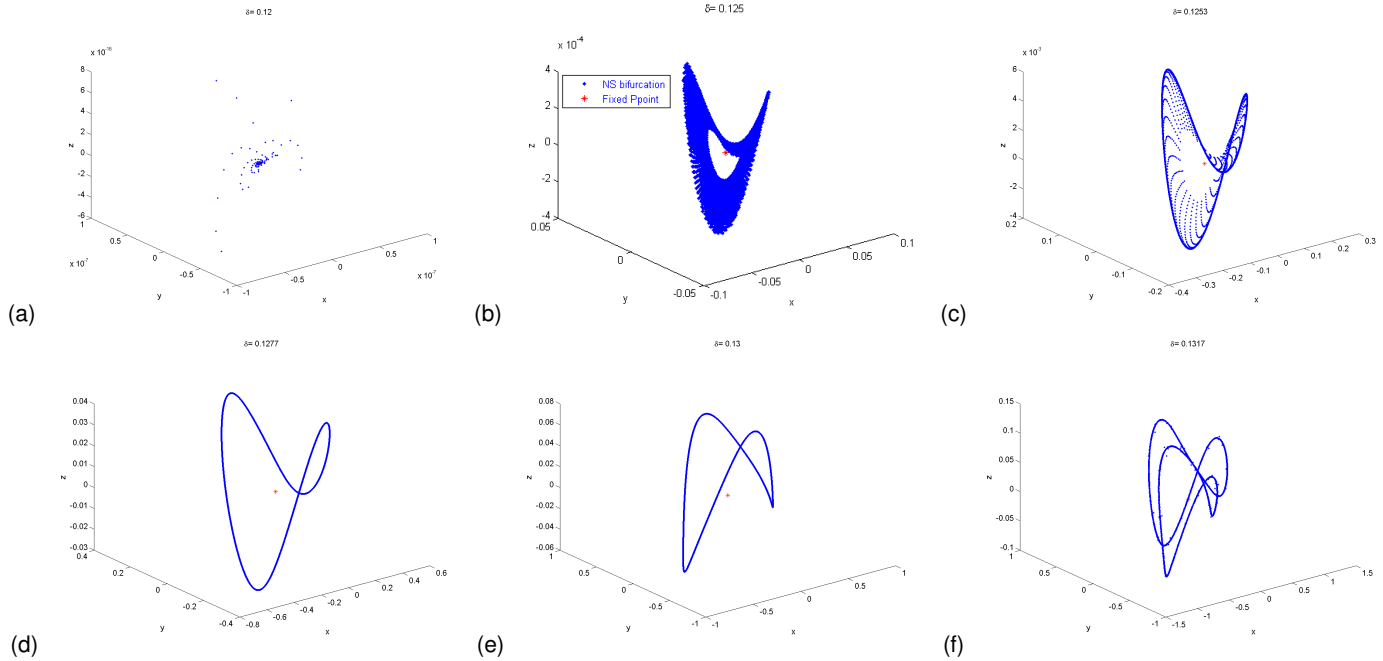

(a) (b) (c)

(d) (e) (f)

Figure 2 Phase portrait for different values of δ connected to Figure 1 a. Red $*$ is the fixed point E_+.

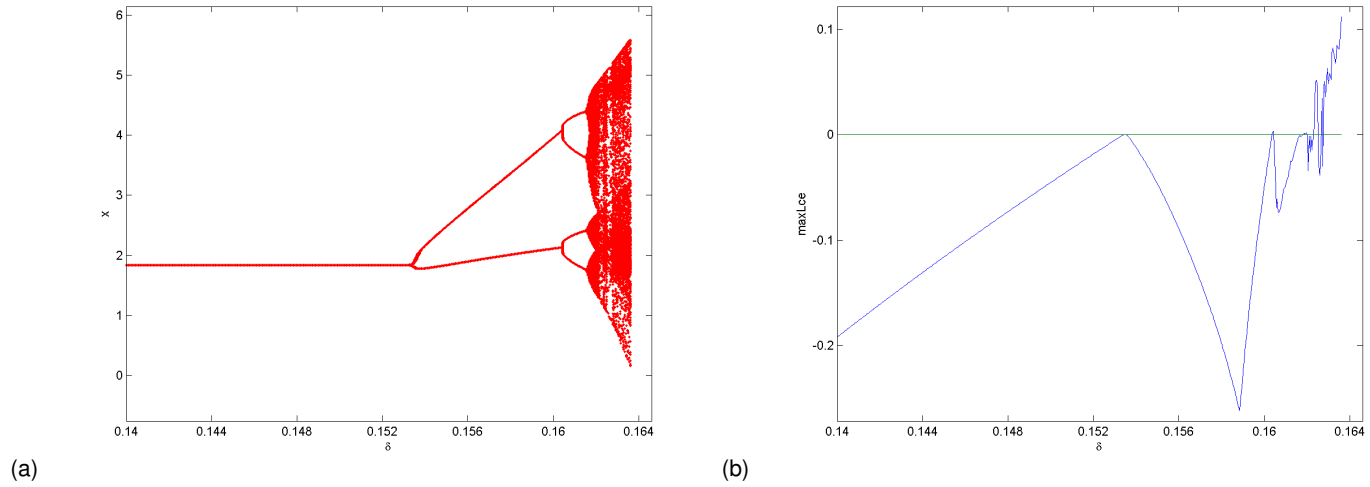

(a) (b)

Figure 3 Flip Bifurcation Diagram: in (a) (δ, x) plane, (b) MLEs, $(x_0, y_0, z_0) = (0.93, 0.93, 0.33)$.

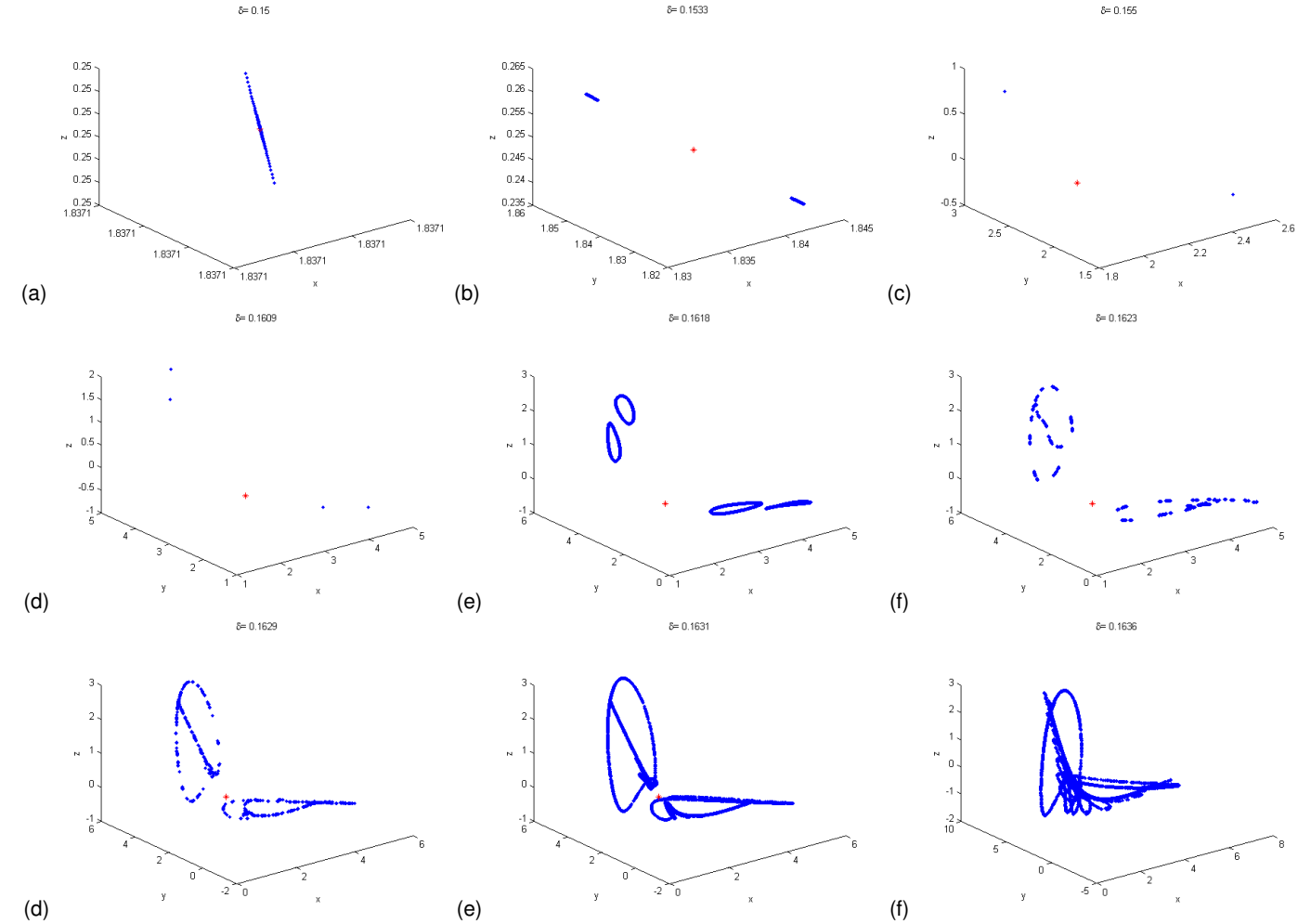

(a) (b) (c)

(d) (e) (f)

(d) (e) (f)

Figure 4 Phase portrait for different values of δ associated to Figure 3 a. Red $*$ is the fixed point E_+.

For $\langle \tau_1, \tau_2 \rangle = 1$, we can take normalized vector as $\tau_2 = \gamma\tau_2$ where, $\gamma = -0.429971 - 1.80561i$. Then

$\tau_1 \sim (0.449192 - 0.489412i, 0.70765, 0.0808016 - 0.226728i)^T, \tau_2 \sim (0.179908 - 0.266131i, 0.636707 + 0.355143i, -0.388348 - 1.63082i)^T$.

Also by (17) the Taylor coefficients are , $\widehat{g}_{20} = 0.216831 + 0.190042i$, $\widehat{g}_{11} = -0.167694 + 0.153913i$, $\widehat{g}_{02} = -0.0967446 - 0.136271i$, $\widehat{g}_{21} = 0.074238 - 0.170412i$.

From (19), we obtain the Lyapunov coefficient $l_2(\delta_{NS}) = -0.094591 < 0$. Therefore, the NS bifurcation is super-critical and the requirements of Theorem 3 are established.

The NS bifurcation diagrams are displayed in Figure 5 (a) which reveal that the condition of stability for the positive fixed point E_+ occurs when $\delta < \delta_{NS}$, loses its stability at $\delta = \delta_{NS_+}$ and there appears an attracting closed invariant curve when $\delta > \delta_{NS}$. The MLEs related to Figure 5 (a) are shown in Figure 5 (b). The non stability of system dynamics are justified with the sign of MLEs.

The phase portraits of system (2) corresponding to diagram of bifurcation shown in Figure 5 (a) are plotted in Figure 6. This figure explicitly illustrate the mechanism of how an invariant smooth closed curve bifurcates from stable fixed point E_+ when δ changes near its critical value. We noticed that NS bifurcations occurs at $\delta = \delta_{NS_+}$ (see in Figure 6(b)). When $\delta > \delta_{NS_+}$, there appears an invariant closed curve and further increasing of δ, NS bifurcation instigate a route to chaos.

Example 4 *Taking parameter values $11.63 \leq a \leq 14.5, 10 \leq c \leq 20.5$, $b = 12, c = 18, \delta = 0.1057$, the two-dimensional parametric space is depicted in Figure 7(a) which shows critical value curves of NS bifurcation of system (2) in (a, c) plane and regions of stability. It may help one to choose parameter values to see how do dynamics of the system change its topological properties. Varying two parameters, multiple bifurcation diagrams of system (2) are plotted in Figure 7(c) together with the sign of MLEs presented in Figure 7(b). We notice that the growth of parameter c delays NS bifurcation.*

In particular, for $c = 18$ the NS bifurcation of system (2) takes place at $a_{NS_+} = 13.999$ around fixed point $E_+ = (1.85193, 1.85193, 0.285803)$. The bifurcation diagram of system (2) with MLEs are plotted in Figure 8 (a,b). The Lyapunov coefficient $l_3(a_{NS_+}) = -0.543329 < 0$ results that the NS bifurcation is super-critical. The phase portraits of system (2) in Figure 9 reflect the break down of invariant closed curve, a period of 9, 11 orbits and attracting chaotic set.

0-1 test algorithm for chaos

The $0-1$ test algorithm (Gottwald and Melbourne 2004; Xin and Li 2013; Xin and Wu 2015) returns a real number $K \in [0, 1]$ and a graph in 2D new coordinates (u, v)-plane.

Let $\widehat{\Phi}(n)$ be finely sampled set of measurement data, where $n = 1, 2, 3, \ldots, N_{tot}$ and N_{tot} is length of data. The test steps are as follows.

Step 1: Take a random real number $d \in \left(\frac{\pi}{5}, \frac{4\pi}{5}\right)$, and define new coordinates $(u_d(n), v_c(n)))$ as follows.

$$\begin{aligned} u_d(n) &= \sum_{j=1}^{n} \widehat{\Phi}(j) \cos(\hat{\theta}(j)) \\ v_d(n) &= \sum_{j=1}^{n} \widehat{\Phi}(j) \sin(\hat{\theta}(j)) \end{aligned} \tag{24}$$

where

$$\hat{\theta}(j) = jd + \sum_{i=1}^{j} \widehat{\Phi}(j), \quad j = 1, 2, 3, \ldots, n$$

Step 2: Define the quantity $SD_d(n)$ called mean square displacement as follows:

$$SD_d(n) = \lim_{N_{tot}\to\infty} \frac{1}{N_{tot}} \sum_{j=1}^{N_{tot}} (u_d(j+n) - u_d(j))^2 + (v_d(j+n) - v_d(j))^2, \tag{25}$$

$$n \in \left[1, \frac{N_{tot}}{10}\right]$$

Step 3: Define the quantity $MSD_d(n)$ called modified mean square displacement as follows:

$$MSD_d(n) = SD_d(n) - \left(\lim_{N_{tot}\to\infty} \frac{1}{N_{tot}} \sum_{j=1}^{N_{tot}} \widehat{\Phi}(j)\right)^2 \frac{1 - \cos nc}{1 - \cos c} \tag{26}$$

Step 4: Define the median value of correlation coefficient K as follows:

$$K = median(\kappa_c) \tag{27}$$

where

$$\kappa_c = \frac{cov(\Omega_1, \Omega_2)}{\sqrt{var(\Omega_1)var(\Omega_2)}} \in [-1, 1]$$

witl vectors $\Omega_1 = (1, 2, 3, \ldots, n_{cut})$, $\Omega_2 = (MSD_d(1), MSD_d(2), MSD_d(3), \ldots, MSD_d(n_{cut}))$, $n_{cut} = round\left(\frac{N_{tot}}{10}\right)$. For the vectors p, s of length n_t, the covariance and variance are defined as follows:

$$\begin{aligned} cov(p, s) &= \tfrac{1}{n_t} \textstyle\sum_{j=1}^{n_t} (p(j) - \bar{p})(s(j) - \bar{s}) \\ \bar{p} &= \tfrac{1}{n_t} \textstyle\sum_{j=1}^{n_t} p(j) \\ var(p) &= cov(p, p) \end{aligned}$$

Step 5: Use the test outputs' interpretation as follows:
(i) $K \approx 0$ suggests that the dynamics of observed data are regular (i.e., periodic or quasi-periodic), whereas $K \approx 1$ suggests that the dynamics of recorded data are chaotic.
(ii) Bounded trajectories in the new coordinate system (p, s) denote regular underlying dynamics, while Brownian-like (unbounded) trajectories denote chaotic underlying dynamics.

Example 5 *The chaotic dynamics (see Figure 9 (a)) of the system (2) are quantified with correlation coefficient value $K = 0.97639$ by $0-1$ test for chaos and the plot in transformed coordinates (p, s) (see Figure 10(b)) showing Brownian-like trajectories. The diagram of correlation coefficient value K is displayed in Figure 10(a) which guarantees that decreasing the values of parameter a causes unstable system dynamics for discrete T system.*

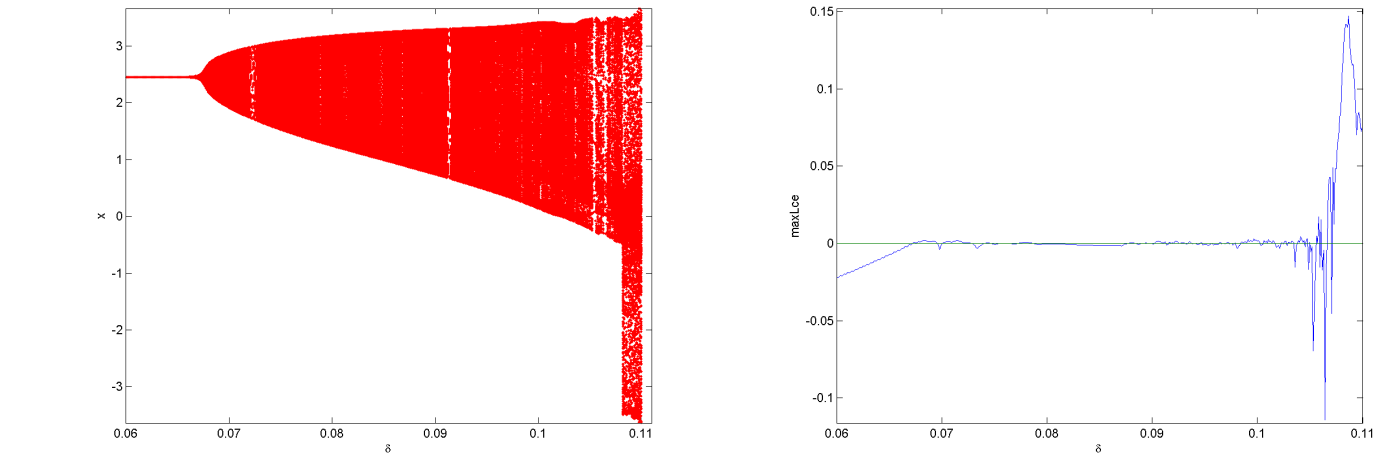

(a) (b)

Figure 5 NS Bifurcation diagram: in (a) (δ, x) plane, (b) MLEs, $(x_0, y_0, z_0) = (0.98, 0.98, 0.6)$.

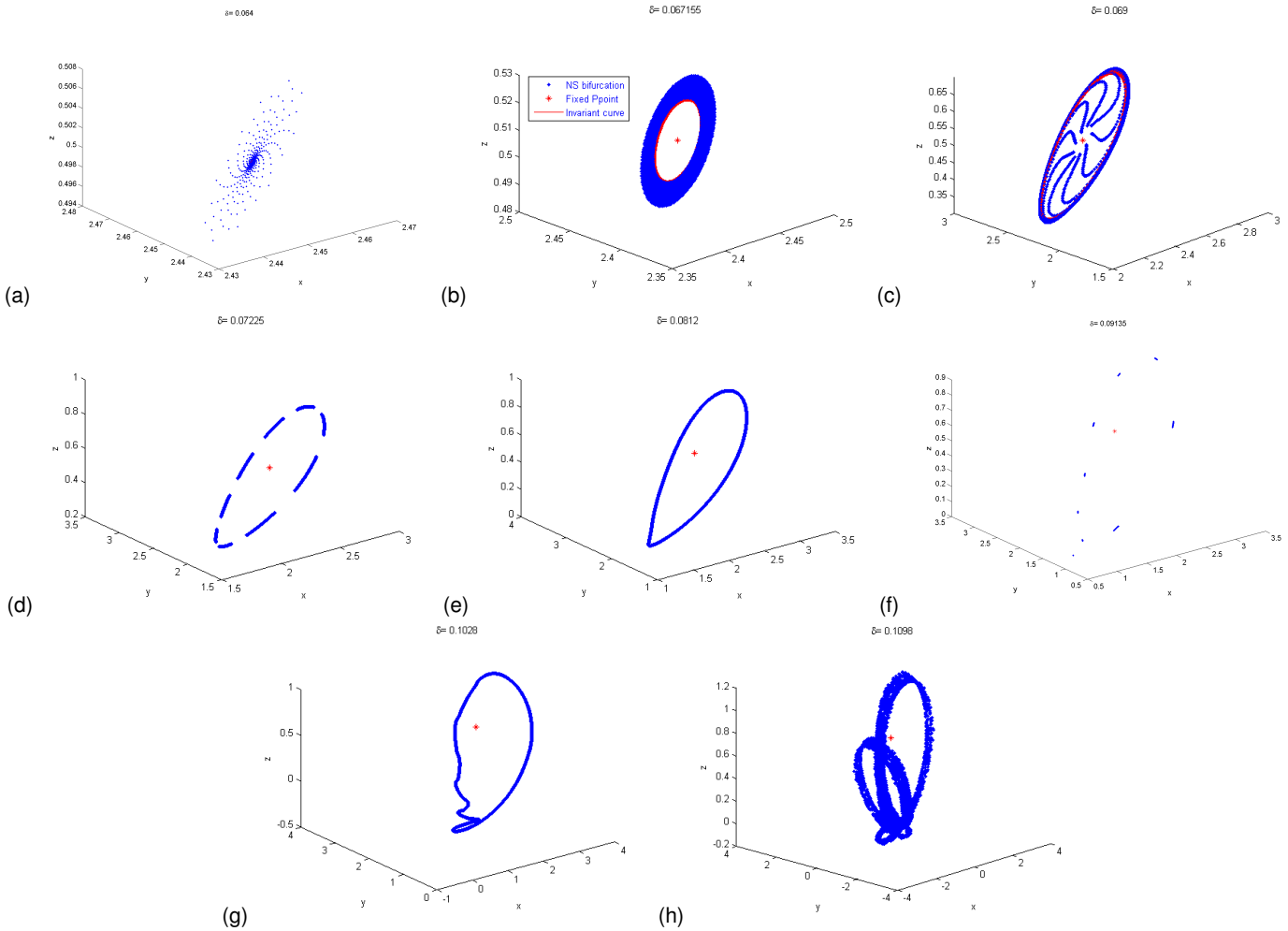

(a) (b) (c) (d) (e) (f) (g) (h)

Figure 6 Phase portrait for different values of δ corresponding to Figure 5 a. Red $*$ is the fixed point E_+.

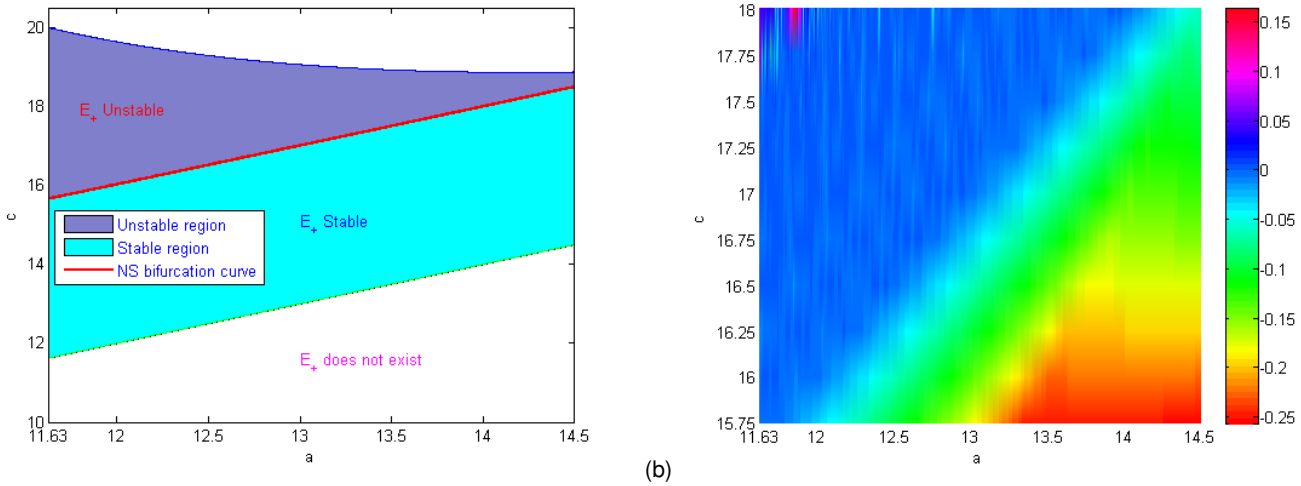

(a) (b)

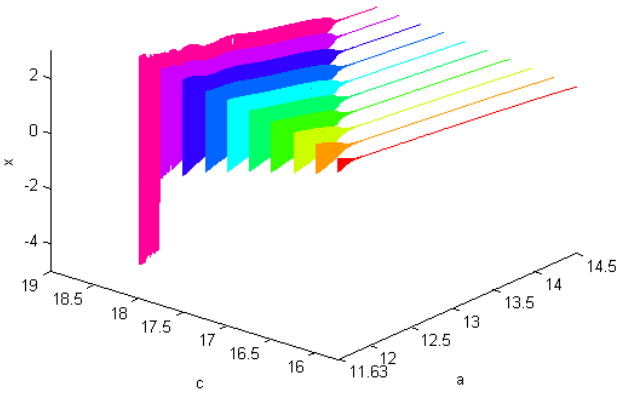

(c)

Figure 7 System Dynamics for two control parameters (a) Stability region in (a, c) plane (b) The projection of MLEs onto (a, c) plane (c) NS bifurcation in (a, c, x) space for $a \in [2.6, 7.5]$ and $c = 3, 3.6, 4.2, 5.04, 6 \in [3, 6]$.

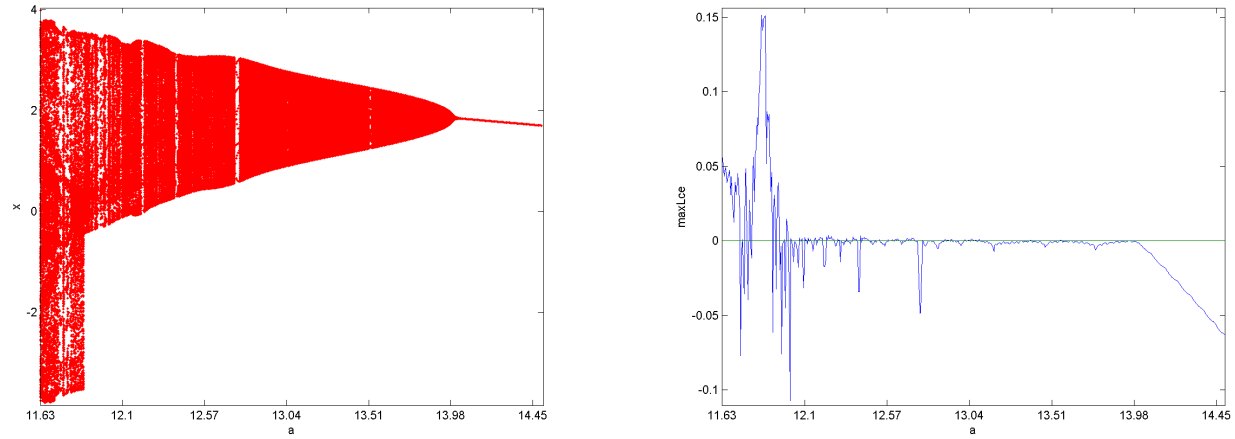

(a) (b)

Figure 8 NS Bifurcation diagram: in (a) (a, x) plane, (b) MLEs, $(x_0, y_0, z_0) = (1.95, 1.95, 1.2)$.

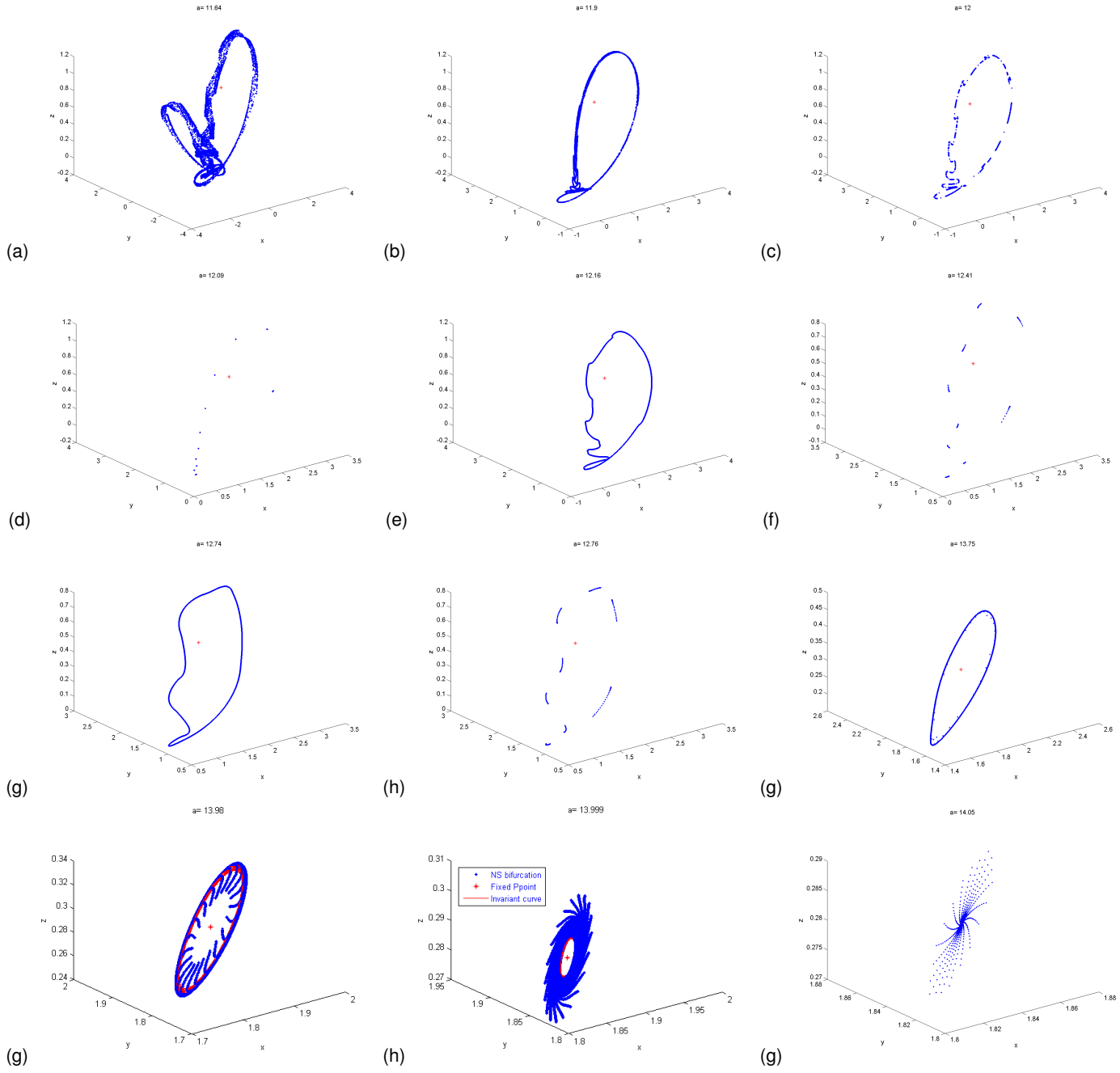

Figure 9 Phase portrait for different values of a corresponding to Figure 8 a. Red $*$ is the fixed point E_+.

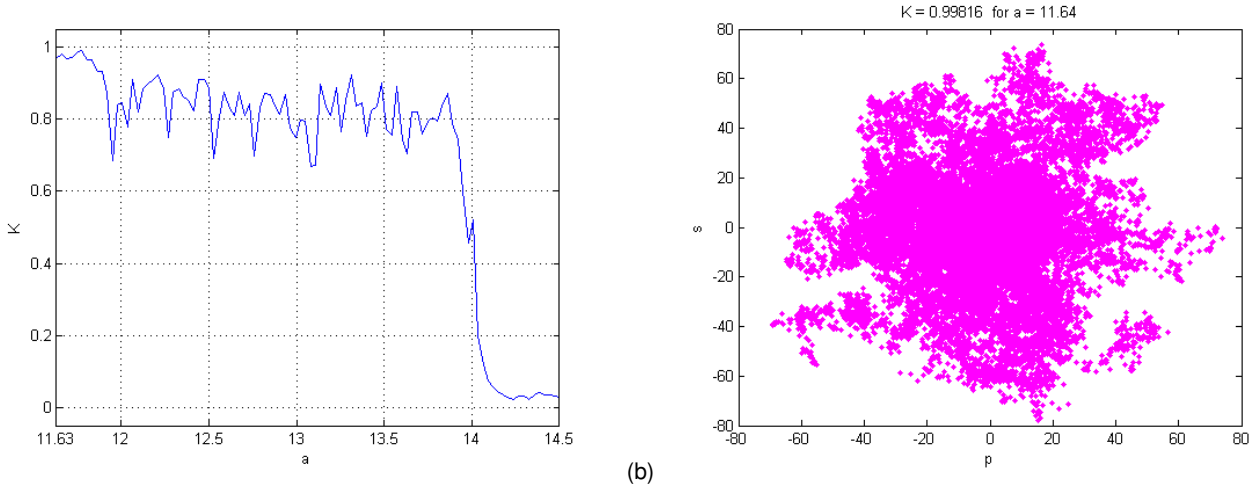

(a) (b)

Figure 10 $0-1$ test for Chaos of system (2). (a) The curve of median of correlation coefficient in (K,δ) plane (b) Dynamics of system (2) in new (p,s) plane.

CHAOS CONTROL

Hybrid control strategy (Yuan and Yang 2015) is applied to system (2) to get the following controlled system

$$\begin{cases} x_{n+1} = \rho\left(x_n + \delta\left(a(y_n - x_n)\right)\right) + (1-\rho)\, x_n, \\ y_{n+1} = \rho\left(y_n + \delta\left((c-a)x_n - a x_n z_n\right)\right) + (1-\rho)\, y_n, \\ z_{n+1} = \rho\left(z_n + \delta\left(x_n y_n - b z_n\right)\right) + (1-\rho)\, z_n \end{cases} \tag{28}$$

For the controlled system (28), at fixed point $E_+ = \left(\sqrt{\frac{b}{a}(c-a)}, \sqrt{\frac{b}{a}(c-a)}, \frac{c-a}{a}\right)$,the zeroes of $|\mu I - J(E_+)|$ (eigenvalues of J) satisfy the equation

$$\mu^3 + \varepsilon_2\mu^2 + \varepsilon_1\mu + \varepsilon_0 = 0. \tag{29}$$

where,

$$\begin{aligned} \varepsilon_2 &= -3 + \delta\rho(a+b), \\ \varepsilon_1 &= 3 - 2a\delta\rho + b\delta\rho(-2 + c\delta\rho), \\ \varepsilon_0 &= -1 - 2a^2 b\delta^3\rho^3 + b\delta\rho(1 - c\delta\rho) + a(\delta\rho + 2bc\delta^3\rho^3) \end{aligned} \tag{30}$$

Lemma 7 *If the fixed point E_+ of the uncontrolled system (2) is unstable, then it is a sink (stable) the controlled system (28), if the roots of (29) lie inside open disk satisfying conditions in Lemma 2.*

Example 6 *To see the effectiveness of hybrid control strategy to control chaotic (unstable) system dynamics, we fix $b = 12, c = 18, \delta = 0.1057$ with $a = 11.64 < a_{NS_+}$. The fixed point $E_+(2.56061, 2.56061, 0.546392)$ of system (2) is then demonstrated to be unstable (see Fig 8), however it is stable for the controlled system (28) iff $0 < \rho < 0.596385$. Taking $\rho = 0.55$, the unstable system dynamics around E_+ are eliminated showing that E_+ is a sink for the controlled system (28) which have been displayed in Figure 11 (a,b). Moreover, for the choice of $\rho = 0.7$, the NS bifurcation moves to negative a-axis and occurs at $a = 12.5042$ for this controlled system by hybrid control strategy (see Figure 11 (c)).*

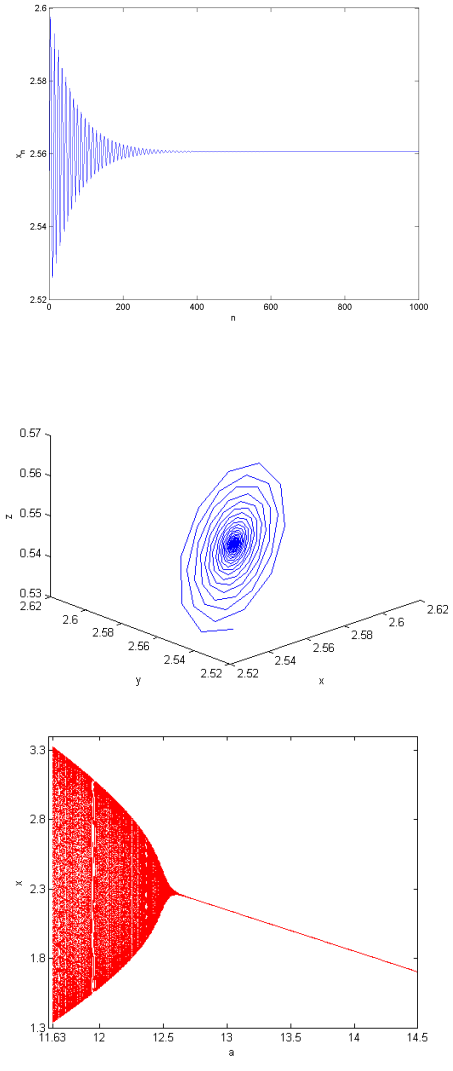

(a) (b) (c)

Figure 11 Dynamics of controlled system (28), (a) Time history of x (b) Phase diagram (c) NS bifurcation in (a,x)-plane for $\rho = 0.7$.

CONCLUSION

We analysis discrete-time chaotic T system both qualitatively and quantitively. The Hopf bifurcation of the T system occurs, and it has an irregular chaotic attractor. We discover that the discrete T system exhibits more varied dynamical behaviors than the continuous system. Firstly, the conditions and directions of NS bifurcation of system (2) around E_0 are explicitly described by center manifold theory. Then we find the criteria of happening Flip and NS bifurcations of system (2) around fixed point E_+.

In addition, we determine directions of these bifurcations. More Specifically, NS bifurcation around E_0 and Flip or NS bifurcation around E_+ take place of system (2) for small perturbation of bifurcation parameter δ or a. Both bifurcations change system dynamics topologically and trigger a route to chaos. For the generation of NS bifurcation, we find closed invariant curve, sudden break down of closed curve, period $-9, -11$ orbits and chaotic attractors when δ and/or a pass their threshold values. For the generation of flip bifurcation, we observe the stable period -1 orbit becomes period $-2, -4$,orbits, 4 closed curves, two-coexisting chaotic sets and nice attracting chaotic set respectively for growth of δ.

Based on two dimensional parameteric space, we see how the mechanism of NS bifurcation switch the behaviors of system and advance or delay of occuring bifurcation when two parameters vary simultaneously. Moreover, for all the cases chaoticity of system dynamics are justified with sign of MLEs and $0-1$ chaos test. Finally, we are able to control and eliminate unstable system trajectories by hybrid control strategy. For this system, it is open to study the other properties like synchronization and co-dimension-2 bifurcation. Studying how two factors affect the dynamics of the discrete T system will be intriguing and difficult, but it is something to keep in mind for future study.

Conflicts of interest

The author declares that there is no conflict of interest regarding the publication of this paper.

Availability of data and material

Not applicable.

LITERATURE CITED

Abdelaziz, M. A., A. I. Ismail, F. A. Abdullah, and M. H. Mohd, 2020 Codimension one and two bifurcations of a discrete-time fractional-order seir measles epidemic model with constant vaccination. Chaos, Solitons & Fractals **140**: 110104.

Babloyantz, A., J. Salazar, and C. Nicolis, 1985 Evidence of chaotic dynamics of brain activity during the sleep cycle. Physics letters A **111**: 152–156.

Camouzis, E. and G. Ladas, 2007 *Dynamics of third-order rational difference equations with open problems and conjectures*, volume 5. CRC Press.

Chakraborty, P., S. Sarkar, and U. Ghosh, 2020 Stability and bifurcation analysis of a discrete prey–predator model with sigmoid functional response and allee effect. Rendiconti del Circolo Matematico di Palermo Series 2 pp. 1–21.

Chen, G., 1999 *Controlling chaos and bifurcations in engineering systems*. CRC press.

Chen, G. and X. Dong, 1998 *From chaos to order: methodologies, perspectives and applications*, volume 24. World Scientific.

Din, Q. and W. Ishaque, 2019 Bifurcation analysis and chaos control in discrete-time eco–epidemiological models of pelicans at risk in the salton sea. International Journal of Dynamics and Control **8**: 132–148.

El Naschie, M., 2003 Non-linear dynamics and infinite dimensional topology in high energy particle physics. Chaos, Solitons & Fractals **17**: 591–599.

Fei, L., X. Chen, and B. Han, 2021 Bifurcation analysis and hybrid control of a discrete-time predator–prey model. Journal of Difference Equations and Applications **27**: 102–117.

Feng, G., D. Yin, and L. Jiacheng, 2021 Neimark–sacker bifurcation and controlling chaos in a three-species food chain model through the ogy method. Discrete Dynamics in Nature and Society **2021**.

Gottwald, G. A. and I. Melbourne, 2004 A new test for chaos in deterministic systems. Proceedings of the Royal Society of London. Series A: Mathematical, Physical and Engineering Sciences **460**: 603–611.

Hu, Z., Z. Teng, and L. Zhang, 2014 Stability and bifurcation analysis in a discrete sir epidemic model. Mathematics and computers in Simulation **97**: 80–93.

Ishaque, W., Q. Din, M. Taj, and M. A. Iqbal, 2019 Bifurcation and chaos control in a discrete-time predator–prey model with nonlinear saturated incidence rate and parasite interaction. Advances in Difference Equations **2019**: 1–16.

Jiang, B., X. Han, and Q. Bi, 2010 Hopf bifurcation analysis in the t system. Nonlinear Analysis: Real World Applications **11**: 522–527.

Kengne, J., Z. Njitacke, and H. Fotsin, 2016 Dynamical analysis of a simple autonomous jerk system with multiple attractors. Nonlinear Dynamics **83**: 751–765.

Khan, A. and M. Javaid, 2021 Discrete-time phytoplankton–zooplankton model with bifurcations and chaos. Advances in Difference Equations **2021**: 1–30.

Khan, M. S., M. Ozair, T. Hussain, J. Gómez-Aguilar, *et al.*, 2021 Bifurcation analysis of a discrete-time compartmental model for hypertensive or diabetic patients exposed to covid-19. The European Physical Journal Plus **136**: 1–26.

Kuznetsov, Y. A., 2013 *Elements of applied bifurcation theory*, volume 112. Springer Science and Business Media, New York, USA.

Li, B. and Q. He, 2019 Bifurcation analysis of a two-dimensional discrete hindmarsh–rose type model. Advances in difference equations **2019**: 1–17.

Li, X.-F., Y.-D. Chu, J.-G. Zhang, and Y.-X. Chang, 2009 Nonlinear dynamics and circuit implementation for a new lorenz-like attractor. Chaos, Solitons & Fractals **41**: 2360–2370.

Liu, Y. and X. Li, 2021 Dynamics of a discrete predator-prey model with holling-ii functional response. International Journal of Biomathematics p. 2150068.

Lorenz, E. N., 1963 Deterministic nonperiodic flow. Journal of atmospheric sciences **20**: 130–141.

Lü, J., G. Chen, and S. Zhang, 2002 Dynamical analysis of a new chaotic attractor. International Journal of Bifurcation and chaos **12**: 1001–1015.

Luo, W., Q. Ou, F. Yu, L. Cui, and J. Jin, 2020 Analysis of a new hidden attractor coupled chaotic system and application of its weak signal detection. Mathematical Problems in Engineering **2020**.

Pecora, L. M. and T. L. Carroll, 1991 Driving systems with chaotic signals. Physical review A **44**: 2374.

Qin, S., J. Zhang, W. Du, and J. Yu, 2016 Neimark–sacker bifurcation in a new three–dimensional discrete chaotic system. ICIC-EL **10**: 1–7.

Rabinovich, M. and H. Abarbanel, 1998 The role of chaos in neural systems. Neuroscience **87**: 5–14.

Rana, S. M. S., 2019a Bifurcations and chaos control in a discrete-time predator-prey system of leslie type. Journal of Applied Analysis & Computation **9**: 31–44.

Rana, S. M. S., 2019b Dynamics and chaos control in a discrete-time ratio-dependent holling-tanner model. Journal of the Egyptian Mathematical Society **27**: 1–16.

Rössler, O. E., 1976 An equation for continuous chaos. Physics Letters A **57**: 397–398.

Sachdev, P. and R. Sarathy, 1994 Periodic and chaotic solutions for a nonlinear system arising from a nuclear spin generator. Chaos, Solitons & Fractals **4**: 2015–2041.

Singh, A. and P. Deolia, 2021 Bifurcation and chaos in a discrete predator–prey model with holling type-iii functional response and harvesting effect. Journal of Biological Systems **29**: 451–478.

Sparrow, C., 2012 *The Lorenz equations: bifurcations, chaos, and strange attractors*, volume 41. Springer Science and Business Media.

Sundarapandian, V., 2011 Global chaos anti-synchronization of tigan and lorenz systems by nonlinear control. Int J Math Sci Appl **1**: 679–690.

Tang, S. and L. Chen, 2003 Quasiperiodic solutions and chaos in a periodically forced predator–prey model with age structure for predator. International Journal of Bifurcation and Chaos **13**: 973–980.

Tigan, G., 2005 Analysis of a dynamical system derived from the lorenz system. Sci. Bull. Politehnica Univ. Timisoara Tomu **50**: 61–72.

Ueta, T. and G. Chen, 2000 Bifurcation analysis of chen's equation. International Journal of Bifurcation and Chaos **10**: 1917–1931.

Vaidyanathan, S. and K. Rajagopal, 2011 Anti-synchronization of li and t chaotic systems by active nonlinear control. In *Advances in Computing and Information Technology: First International Conference, ACITY 2011, Chennai, India, July 15-17, 2011. Proceedings*, pp. 175–184, Springer.

Wen, G., 2005 Criterion to identify hopf bifurcations in maps of arbitrary dimension. Physical Review E **72**: 026201.

Xin, B., T. Chen, and J. Ma, 2010 Neimark-sacker bifurcation in a discrete-time financial system. Discrete Dynamics in Nature and Society **2010**.

Xin, B. and Y. Li, 2013 0-1 test for chaos in a fractional order financial system with investment incentive. In *Abstract and Applied Analysis*, volume 2013, Hindawi.

Xin, B. and Z. Wu, 2015 Neimark–sacker bifurcation analysis and 0–1 chaos test of an interactions model between industrial production and environmental quality in a closed area. sustainability **7**: 10191–10209.

Yang, T. and L. O. Chua, 1997 Impulsive stabilization for control and synchronization of chaotic systems: theory and application to secure communication. IEEE Transactions on Circuits and Systems I: Fundamental Theory and Applications **44**: 976–988.

Yao, S., 2012 New bifurcation critical criterion of flip-neimark-sacker bifurcations for two-parameterized family of-dimensional discrete systems. Discrete Dynamics in Nature and Society **2012**.

Yong, C. and Y. Zhen-Ya, 2008 Chaos control in a new three-dimensional chaotic t system. Communications in Theoretical Physics **49**: 951.

Yuan, L.-G. and Q.-G. Yang, 2015 Bifurcation, invariant curve and hybrid control in a discrete-time predator–prey system. Applied Mathematical Modelling **39**: 2345–2362.

Zhang, Y., Q. Cheng, and S. Deng, 2022 Qualitative structure of a discrete predator-prey model with nonmonotonic functional response. Discrete & Continuous Dynamical Systems-S .

Zhao, M., 2021 Bifurcation and chaotic behavior in the discrete bvp oscillator. International Journal of Non-Linear Mechanics **131**: 103687.

How to cite this article: Rana, S., S. Bifurcation Analysis and 0-1 Chaos Test of a Discrete T System. *Chaos Theory and Applications*, 5(2), 90-104, 2023.